LOCALIZING AND CHARACTERIZING SINGLE FIBER POPULATIONS THROUGHOUT THE BRAIN

Chantal M.W. Tax[1], Dmitry S. Novikov[2], Eleftherios Garyfallidis[3], Max A. Viergever[1], Maxime Descoteaux[3], and Alexander Leemans[1]

[1]*Image Sciences Institute, University Medical Center Utrecht, Utrecht, Utrecht, Netherlands,* [2]*Center for Biomedical Imaging, New York University School of Medicine, New York, New York, United States,* [3]*Sherbrooke Connectivity Imaging Lab, Université de Sherbrooke, Sherbrooke, Quebec, Canada*

Purpose Diffusion MRI can measure the diffusion process of water particles to infer information on tissue microstructure and architecture. While a lot of attention has been given to the so called "crossing fibers problem" in the brain, many fundamental questions on the microstructure in "single fiber population (SFP) configurations" remain still unanswered. Studying SFPs can infer information on its organization into distinct fiber compartments[1,2], on our ability to measure microstructural parameters like axon diameter[3] and amount of myelin, and on the choice of an appropriate response function (RF) for spherical decovolution (SD)[4,5], amongst others. Although many diffusion MRI methods define one typical SFP for the whole brain (mostly in the corpus callosum (CC)), it is well known that the properties of SFPs vary throughout the brain[1,2,3,6]. In this work, we investigated the spatial distribution and characteristics of SFPs as measured by multi-shell diffusion MRI.

Methods Data and preprocessing: We used the extensive MASSIVE dataset[7] and extracted 5 shells (125, 250, 250, 250 and 300 directions on the half sphere with b-values of 500, 1000, 2000, 3000 and 4000 s/mm^2), and 204 b=0 s/mm^2 images. The dataset was collected using SE-EPI with the following parameters: TE/TR: 100/7500 ms; voxel size: 2.5x2.5x2.5 mm3; G_{max}: 61.9 mT/m; Δ/δ: 51.6/32.8 ms; Images were corrected for subject motion and eddy currents using ExploreDTI[8].

SFP localization by multi-shell recursive CSD calibration: Previous work used constrained SD (CSD) on single-shell data to recursively calibrate the RF in the brain[4]. In each iteration, this approach calculates an "improved" RF by taking the mean of voxels that contain only one genuine fiber orientation distribution (fODF) peak, based on CSD with the RF of the previous iteration. Voxels with ratio second fODF peak / first fODF peak smaller than a preset peak ratio threshold t (here, $t = 0.01$) are considered as "SFP voxels". By looking at the voxels that are used for the *final* RF, one can create an SFP mask. To fully exploit b-value dependency, we used the recursive calibration to create an SFP mask *for every shell* (Fig. 1a). A final SFP mask was created by taking the intersection of the SFP masks over all shells (Fig. 1b).

SFP characterization (raw signal): The signals of all SFP voxels were rotated so that the fODF peak (CSD on the b=4000 s/mm^2 shell) coincides with the z-axis. Signals were interpolated (trilinear) to determine the signal decay in the direction parallel and perpendicular to the fiber. The biexponential model with two non-exchanging compartments (slow and fast diffusion) was fitted to the parallel and perpendicular signal decay curves.

SFP characterization (model features): The following 3D reconstruction methods were fitted on the relevant MASSIVE data using Dipy[9] and ExploreDTI[8]: diffusion tensor imaging (DTI) (b=1000 s/mm^2 shell), diffusion kurtosis imaging (DKI) (b=500, 1000 and 2000 s/mm^2 shells), CSD (b=4000 s/mm^2 shell), and 3D Simple Harmonic Oscillator based Reconstruction and Estimation (3D-SHORE, all shells)[10]. For each reconstruction method, relevant (microstructural) features of the voxels in the SFP mask were computed (see table 1). To be able to extract more tract-specific information, SFP voxels were considered to belong to a particular tract if they intersected with the tract mask generated from deterministic tractography (CSD on the b=4000 shell), see table 1.

Results Fig. 1a shows that the number of voxels identified as SFP voxels decreases with b-value due to higher angular resolution. Fig. 1b shows the final SFP mask with SFPs located in the CC, optic radiation, cerebellar peduncle, fornix, and internal capsule, amongst others. Fig. 2a shows the 3D mean SFP signal decay (spherical harmonic fit on each shell), whereas Figs. 2b and 2c show respectively the signal decays of each individual voxel in the direction parallel and perpendicular to the fiber. The decay is clearly non-monoexponential in both directions: Fig. 3 shows a biexponential fit with parameter estimates for the slow and fast compartments, indicating that diffusion coefficients differ between compartments in a given direction (contrary to some assumptions in literature[11,12]). Table 1 shows that microstructural features of SFPs do vary between tracts: The SLF, for example, has a relatively low RD compared to other tracts and the SFP average.

Discussion and Conclusion In this work we have localized SFP voxels by recursively excluding crossing fiber voxels with CSD. Only if fODFs *across all shells* exhibit a single peak, the voxel is considered an SFP voxel. In future work we will further explore the effect of this condition, e.g. by simultaneously calibrating the RF on all shells using multi-shell CSD[13]. We have investigated the average signal decay over all SFPs parallel and perpendicular to the fiber. At this point, it is problematic to assign the compartments to intra- and extra-axonal space since the estimated fractions of the decay curves are not consistent among both directions, possibly due to averaging of SFPs throughout the brain. We have extracted features for SFPs in different tracts. By computing mean indices only from SFPs in a tract instead of averaging over all voxels, the results are to a lesser extent biased by crossing fiber voxels and other partial volume effects. This can reveal potential between-tract or between-subject differences that might otherwise remain undetected. The computed indices can be used as reference for healthy brain in group studies or simulation studies. In future work wider range of models and descriptive features can be estimated in these SFPs.

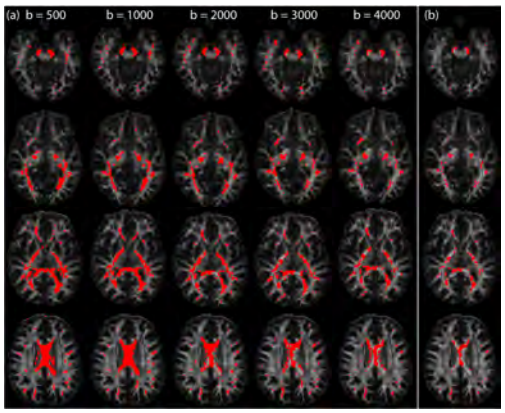

Fig. 1: (a) SFP masks overlaid on FA map for each shell. (b) Final SFP mask is the intersection of all single shell SFP masks.

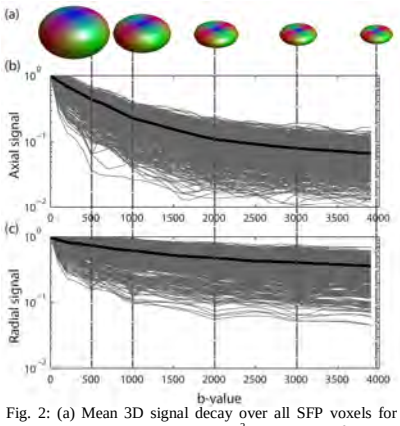

Fig. 2: (a) Mean 3D signal decay over all SFP voxels for b = [500, 1000, 2000, 3000, 4000] s/mm^2. Signal decay for individual voxels (grey) and mean (black) in the direction parallel (b) and perpendicular (c) to the fiber.

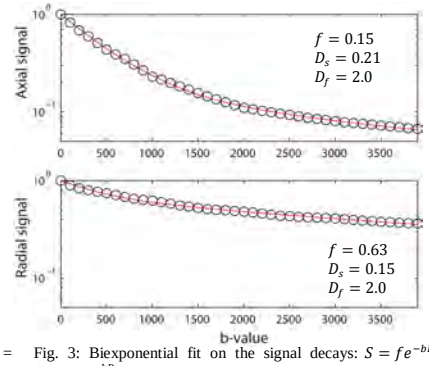

Fig. 3: Biexponential fit on the signal decays: $S = fe^{-bD_s} + (1-f)e^{-bD_f}$ with D_s and D_f the slow and fast diffusivities in $\mu m^2/ms$.

Model		DTI								DKI									CSD	SHORE	
Measure		FA	AD	RD	C_l	C_p	C_s	RA	MD	AK	KA	MK	AM	AWF	AEAD	READ	RK	TORT	AFD	RTOP	MSD
SFP mask	Mean	.61	1.7e-3	6.0e-4	.62	.080	.30	.40	9.6e-4	.60	.34	1.1	.92	.38	1.4e-3	3.1e-3	1.5	2.2	1.4	5.8e5	1.5e-4
CC splenium	Mean	.59	1.8e-3	6.8e-4	.62	.073	.31	.40	1.0e-3	.57	.31	1.0	.93	.37	3.3e-3	1.5e-3	1.4	2.4	1.5	5.2e5	1.7e-4
CST	Mean	.63	1.6e-3	5.4e-4	.63	.11	.27	.43	9.0e-4	.62	.36	1.2	.89	.40	3.1e-3	1.4e-3	1.6	2.3	1.4	7.0e5	1.4e-4
SLF	Mean	.59	1.4e-3	4.9e-4	.61	.10	.30	.39	8.1e-4	.65	.37	1.1	.90	.40	2.6e-3	1.2e-3	1.7	2.1	1.5	6.2e5	1.4e-4
CC genu	Mean	.61	1.7e-3	5.6e-4	.65	.051	.30	.41	9.5e-4	.57	.34	1.0	.97	.38	3.0e-3	1.4e-3	1.5	2.2	1.3	5.6e5	1.5e-4
CG	Mean	.62	1.6e-3	5.2e-4	.65	.054	.29	.42	8.8e-4	.62	.37	1.1	.96	.40	2.9e-3	1.3e-3	1.6	2.2	1.3	5.9e5	1.4e-4

Table. 1: Model features in SFP voxels: FA: fractional anisotropy, AD: axial diffusivity [mm^2/s], RD: radial diffusivity [mm^2/s], C_l: linear, C_p: planar, C_s: spherical coefficients, RA: relative anisotropy, MD: mean diffusivity [mm^2/s], AK: axial kurtosis, KA: kurtosis anisotropy, MK: mean kurtosis, AM: mode of anisotropy, AWF: axonal water fraction[2], AEAD: axial extra-axonal diffusivity [mm^2/s], READ: radial extra-axonal diffusivity [mm^2/s], RK: radial kurtosis, TORT: tortuosity, AFD: apparent fiber density, RTOP: return-to-origin probability, MSD: mean squared displacement. Fiber tracts: CC splenium: occipital projections of corpus callosum, CST: corticospinal tract, SLF: superior longitudinal fasciculus, CC genu: frontal projections of the corpus callosum, CG: cingulum

References

[1] Fieremans et al, NBM 23:711, 2010; [2] Fieremans et al, NeuroImage 58:177, 2011; [3] Assaf et al, MRM, 59(6):1347-54, 2008; [4] Tournier et al, NeuroImage 35:1459-1472, 2007; [5] Tax et al, NeuroImage, 86:67-80, 2014; [6] Reisert et al, MICCAI Part III, LNCS 8675, pp. 201–208, 2014; [7] Froeling et al, ISMRM 2582, 2014; [8] www.ExploreDTI.com; [9] Garyfallidis et al, Front Neuroinform 8:8, 2014; [10] Merlet et al, Med Image Anal 17(5):556-72, 2013; [11] Panagiotaki et al, NeuroImage 59(3):2241-54, 2012; [12] Zhang et al, NeuroImage 61(4):1000-16, 2012; [13] Jeurissen et al, NeuroImage (in press);